JOURNAL OF APPLIED ELECTROCHEMISTRY 26 (1996) 721–732

Electrosynthesis of a manganese(III) aminopolycarboxylate complex in alkaline media

E. L. GYENGE, C. W. OLOMAN

Department of Chemical Engineering, University of British Columbia, Vancouver, BC, V6T 1Z4, Canada

Received 7 July 1995; revised 18 January 1996

Mn(III)CyDTA [(*trans*-cyclohexane-1,2-diamine-*N*,*N*,*N*′,*N*′-tetraacetato) manganate(III)] was generated electrochemically from Mn(II)CyDTA (6–54 mM) in 0.1 M $NaHCO_3$ at pH 9.0 and 10.5, respectively, 25 °C, for two CyDTA/Mn molar ratios (1/1 and 2/1). A divided batch electrochemical reactor was employed with anode current densities from 2.6 to 102 A m^{-2}. Separate cyclic voltammetry experiments of Mn(III)CyDTA in alkaline media showed a prepeak behaviour, indicating the adsorption of Mn(II) species. The visible anodic deposit, formed during the electrosynthesis of Mn(III)CyDTA at pH 10.5 and 1/1 CyDTA/Mn molar ratio on stainless steel and PbO_2/Pb, reduces the current efficiency for Mn(III). For a Mn(II) concentration of 18 mM and at 13 A m^{-2}, the graphite and platinized titanium anodes gave a current efficiency for Mn(III) of 78% and 66%, respectively, without a visible deposit. A 2/1 CyDTA/Mn molar ratio, avoided a visible anodic deposit formation, but gave lower current efficiencies for Mn(III) than in the case of a 1/1 ligand to metal ratio. The electrosynthesis of Mn(III)CyDTA is recommended for routine preparation of the complex and is also suitable for *in situ* electrochemically mediated oxidations in alkaline media (up to pH 11).

1. Introduction

Due to the hydrolysis and disproportionation of the Mn(III) ion in aqueous alkaline media [1], both the synthesis and applications as an oxidant of the uncoordinated Mn(III) are limited to strong acidic slurries and solutions (usually pH < 0). The electrochemical generation of Mn(III) salts in strong acidic media has been extensively investigated. These studies have been partly triggered by the subsequent employment of Mn(III) as an oxidant, in a variety of indirect electroorganic reactions [2]. The oxidation of $MnSO_4$ to $Mn_2(SO_4)_3$ has been investigated in H_2SO_4 solutions and slurries on anodes such as PbO_2/Pb [3, 4], Pt [4–6] and graphite [4]. The current efficiencies for Mn(III) were between 65 to 90%, depending on the conditions employed. Comninellis and Plattner found that the Ag(I) ion catalyses the electrolytic oxidation of Mn(II) to Mn(III) on Pt in H_2SO_4 (15–17 M), giving an almost 100% current efficiency for Mn(III) at a current density of 250 A m^{-2} and 80 °C [5]. The electrochemically generated $Mn_2(SO_4)_3$ was employed in the indirect electrochemically mediated oxidation of various organic compounds such as *p*-xylene [3], aniline [8] and 4,4′-bibenzoanthrone [6].

A voltammetric study of the Mn(II) oxidation to Mn(III) on platinum and glassy carbon electrodes in 6.15 M H_2SO_4, revealed that the Mn(II) oxidation was controlled by anodic film formation [9]. The anodic deposition was also responsible for a significant drop in the current efficiency for Mn(III) during the electrolytic oxidation of $MnSO_4$ (20 g dm^{-3}) slurried in H_2SO_4 (200 g dm^{-3}) on PbO_2/Pb at current densities higher than 4300 A m^{-2} [4]. The anode deposit hindered the transport of Mn(II) to the electrode surface, causing a drop of current efficiency for Mn(III).

Besides the applications of Mn(III) as a strong oxidant in acidic media ($E^{\circ}_{Mn(III)/Mn(II)} \sim 1.5$ V vs SHE at pH < 0, 25 °C [10]), there is a need for oxidizing agents capable to carry out various oxidation reactions in aqueous alkaline media. A few examples of such reactions are the catalytic oxygen bleaching of wood pulp [11–13] and the redox reactions of certain biologically relevant compounds, for example, thiols [14, 15]. Furthermore, if the oxidizing agent could be electrochemically generated directly in alkaline media, then *in situ* electrochemically mediated high pH oxidations could be performed. Complex formation is the only way to stabilize the Mn(III) ion in aqueous alkaline media. However at pH above 9 most manganese complexes are decomposed and precipitated as hydroxo species [12]. In addition to manganese porphyrin and phthalocyanine complexes [16], the complex of Mn(III) with *trans*-cyclohexane-1,2-diamino-*N*,*N*,*N*′,*N*′-tetraacetic acid (CyDTA) has been reported to be stable up to pH 11 at 25 °C [17]. The greater stability of the CyDTA complex compared with analogous EDTA complexes, is due to the inflexibility of the cyclohexane ring [18]. Unfortunately, by complexation the oxidizing power of Mn(III) is diminished ($E^{\circ}_{\{Mn(III)/Mn(II)\}CyDTA} = 0.814$ V vs SHE at pH 4, 25 °C [17]). On top of this, it is well known that the transition metal-EDTA type ligand equilibria is pH dependent [19] and in alkaline media a further decrease of the reduction potential of Mn(III)CyDTA is expected. Nevertheless, Mn(III)CyDTA is a versatile

0021-891X

oxidant in aqueous media, for a wide range of pH (between 2 and 10.5), being employed for instance in the oxidation of oxalate [20], thiols and thiol containing organic compounds [14, 15] and recently in the oxidative delignification of the kraft pulp [21].

The chemical synthesis of Mn(III)CyDTA, developed by Hamm and Suwyn [17], is based on the oxidation at 0 °C of $Mn(NO_3)_2$ (or $MnSO_4$) by MnO_2 in a slurry containing the ligand CyDTA in a 2/1 CyDTA/Mn molar ratio. After 1 h, the remaining MnO_2 is filtered off and Mn(III)CyDTA is crystallized from the filtrate. The yield from this procedure is 80% [17].

Regarding the electrochemical preparation of any Mn(III) complex, there is relatively little published information. Cui and Dolphin reported the electrosynthesis of Mn(III)-malonate on a glassy carbon anode in a divided cell at pH 4.5 [22]. The resulting Mn(III)-malonate was used in studies related to the biodegradation of lignin. Bath and Sherigara prepared Mn(III)-acetate by electrochemical oxidation of $Mn(OAc)_2$ (above 50 mM) in aqueous acetic acid (AcOH) [23]. They carried out the electrolysis in a differential area, undivided cell, using a platinum foil anode. The highest current efficiency for Mn(III) was 79% at an anode current density of $10\,A\,m^{-2}$. Bhat and Sherigara employed the Mn(III)-acetate in the oxidation of vitamin B_6 [23].

The goal of the present work was the investigation of the electrochemical synthesis of Mn(III)CyDTA under various experimental conditions (e.g., pH, CyDTA/Mn molar ratio, Mn(II) concentration, current density) with regard to its application in the *in situ* electrochemically mediated delignification of wood pulp in alkaline media. The adsorption of manganese species and the pH dependency of the Mn(III)CyDTA electrochemical behaviour was also studied by means of cyclic voltammetry.

2. Experimental apparatus and procedures

2.1. *Cyclic voltammetry*

The cyclic voltammetry equipment consisted of a Pine potentiostat (RDE3), a Goldstar DM-7241 digital multimeter, employed in the high impedance voltmeter mode and a Watanabe X–Y recorder (WX 446). The following working electrodes were used: graphite disc ($A = 0.33\,cm^2$), platinum wire ($A = 0.76\,cm^2$) and stainless steel (316) wire ($A = 0.34\,cm^2$). The counter electrode was a platinized titanium plate ($A = 10.4\,cm^2$). A saturated calomel reference electrode (SCE, Fisher Scientific) was also employed, together with a Luggin capillary.

To assure a clean electrode surface, before each measurement the working electrodes were subjected to a mechanical followed by an electrochemical pretreatment [24]. Oxygen was eliminated from the electrolyte by purging nitrogen for 5 to 10 min. The actual cyclic voltammetry measurement always started with the recording of the background current from the supporting electrolyte, which was 1 M KCl or 1 M KCl and 0.1 M $NaHCO_3$.

For the cyclic voltammetric investigations the Mn(III)CyDTA was prepared according to the chemical method developed by Hamm and Suwyn [17]. The Mn(III)CyDTA concentration in the supporting electrolyte was 0.092 mM. The cyclic voltammograms were recorded at 20 or 25 °C, for different scan rates in the range of 33 to $167\,mV\,s^{-1}$. In all runs the nth scan ($n > 1$) was recorded. The pH of the electrolyte was gradually changed by addition of 2 M NaOH, to study the effect of pH on the electrochemical behaviour of Mn(III)CyDTA.

2.2. *Laboratory electrochemical reactor and preparation of the anolyte*

For the electrosynthesis of Mn(III)CyDTA in alkaline media, a cylindrical, divided batch electrochemical reactor was employed (Fig. 1).

The reactor, made of Plexiglas, was divided in two chambers of 1 litre effective volume each, by a cation exchange membrane (Nafion® 324), held between two perforated Plexiglas supporting plates. The anolyte was stirred at 2800 rpm with a laboratory stirrer (Talboys Inc.) using an axial flow impeller. The electrodes were connected to a digital DC power supply (Xantrex) with output voltage between 0 to 15 V and output current from 0 to 4 A. All

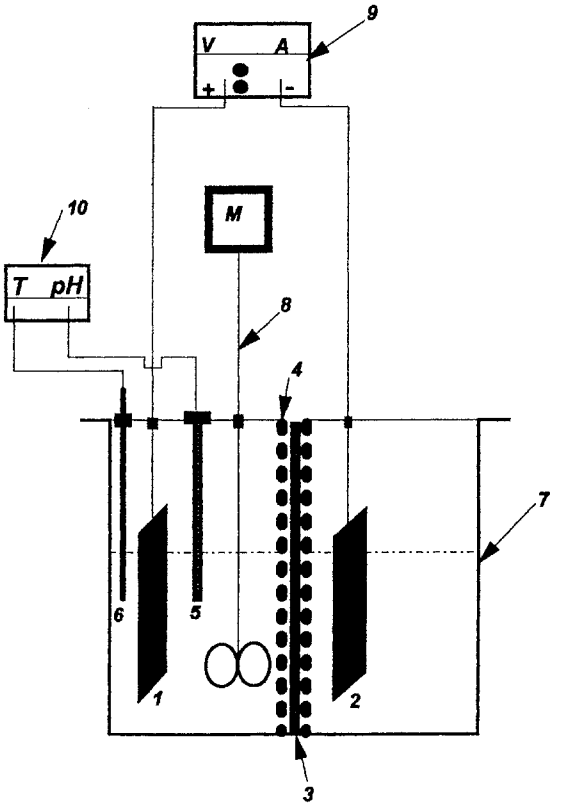

Fig. 1. The divided, batch electrochemical reactor employed in the electrosynthesis of Mn(III)CyDTA. Legend: (1) anode, (2) cathode, (3) cation exchange membrane, Nafion® 324, (4) perforated supporting plates, (5) pH electrode, (6) ATC (temperature probe), (7) electrochemical reactor, (8) mixer, (9) d.c. power supply and (10) '3 in 1' pH meter.

electrosynthesis runs were performed under galvanostatic conditions. The usual electrosynthesis time was 1 h and the temperature 25 °C.

The following six anodes were investigated: stainless steel (316) screen with a wire diameter of 0.51 mm and 20 openings per inch ($A = 232\,cm^2$), stainless steel plate (316) ($A = 71\,cm^2$), graphite plate ($A = 58\,cm^2$), platinized titanium plate ($A = 71\,cm^2$), nickel plate ($A = 56\,cm^2$) and lead plate ($A = 56\,cm^2$).

The cathode in all runs was a platinized titanium plate ($A = 70\,cm^2$). The catholyte was a NaOH solution at pH 13.5. Both sides of the electrodes were exposed to the electrolyte.

Due to the precipitation of the Mn(II) ion in aqueous alkaline media as $Mn(OH)_2$, the anolyte has to be carefully prepared. Thus, the following procedure was developed. A 0.1 M $NaHCO_3$ solution in distilled water was prepared. The pH of this solution was set to about 11 by adding 2 M NaOH. The resulting bicarbonate solution was placed in the anode chamber of the electrochemical reactor. The desired amount of ligand, CyDTA (Aldrich Chemical Corp. Inc.) was added under vigorous mixing at 25 °C, followed by the addition of $MnSO_4 \cdot H_2O$ (BDH Inc.). After adjusting the pH to the desired value, 10.5 or 9.0, by addition of 2 M NaOH, the electrolysis was started. It must be emphasized that the order in which the chemicals are added in this procedure is very important. For instance, if the pH of the bicarbonate solution is not increased to 11, when the ligand CyDTA is added, the pH drops to about 4 or 5. At this pH the HCO_3^- decomposes. If under these conditions the $MnSO_4$ is added and the pH is increased to 10.5, an intensive precipitation occurs. The dark brown precipitate composed of manganese hydroxides and oxides, makes the electrosynthesis impossible. Thus, the HCO_3^- besides its role as a supporting electrolyte, contributes to the stabilization of the manganese ions.

The pH was measured with a Beckman Instrument Co. glass electrode, connected to a Cole–Parmer pH meter (pH-vision 6071). The pH of the anolyte in some experiments was controlled by measuring it each 15 min and adjusting it to the desired value by addition of a 2 M NaOH solution.

By performing repeated experiments under the same conditions the following standard deviations were obtained: for current efficiency ±3%, for Mn(III) concentration ±0.08 mM.

2.3. *Qualitative and quantitative analysis of Mn(III)CyDTA*

At the end of the electrosynthesis the anolyte was acidified with 50 ml glacial AcOH. A sample at pH 4.5 was withdrawn from the anode chamber and its absorption spectra was recorded in the range of 200 to 900 nm. A Varian 2000 spectrophotometer was employed with a scanning speed of $2\,nm\,s^{-1}$. The spectra of the anolyte sample showed a single, broad peak between 480 to 518 nm, matching perfectly the spectra of the chemically synthesized Mn(III)CyDTA and the Mn(III)CyDTA absorption spectra from the literature [14, 17].

The trivalent manganese was quantitatively determined by an iodometric method based on the reduction of Mn(III) in acetic acid media by KI and the titration of the separated iodine with sodium thiosulfate [25, 26].

3. Results and discussion

3.1. *Cyclic voltammetry study of Mn(III)CyDTA*

The first investigation was performed on the graphite disc working electrode in a 1 M KCl supporting electrolyte at pH 8.0, 25 °C. The Mn(III)CyDTA concentration was 0.092 mM and the CyDTA/Mn molar ratio was 2/1. Under these conditions the Mn(III)CyDTA exhibited no peak response in the potential range of +0.7 V vs SCE to −0.5 V vs SCE (Fig. 2).

Other authors have also found no peak responses for manganese under certain experimental conditions. For instance, Landucci reported the absence of cyclic voltammetry response for Mn(II) on a carbon electrode in the presence of EDTA in borax solution at pH 9.0 [27]. Similarly, both Mn(II) 5-sulfonatosalicylate and manganese cyanide showed no anodic or cathodic waves on a graphite electrode at pH 9.4, in a borate buffer and 3.75/1 ligand to metal ratio [12]. Comninellis *et al.* have found that in 88% H_2SO_4, on a Pt electrode for a benzoic acid/Mn(II) molar ratio greater than 1/2, both the reduction peak of Mn(III) and the oxidation peak of Mn(II) disappeared [2].

The absence of Mn(III)CyDTA cyclic voltammetry response under the conditions presented in Fig. 2, can be explained by looking at the structure of the complex. The Mn(III) ion forms a seven-coordinated, 1 : 1 complex with CyDTA, where six sites are occupied by the CyDTA itself, while the seventh by a water molecule or other species (e.g., OH^-) [17]. It is known that in the case of transition metal-aminopolycarboxylate complexes, the cyclic voltammetry peak currents disappear when the ligand to metal ratio exceeds the equivalence point corresponding to the complex stoichiometry (i.e., usually 1 : 1) [28]. The employment of a 2/1 CyDTA/Mn molar ratio exceeds the stoichiometric equivalence

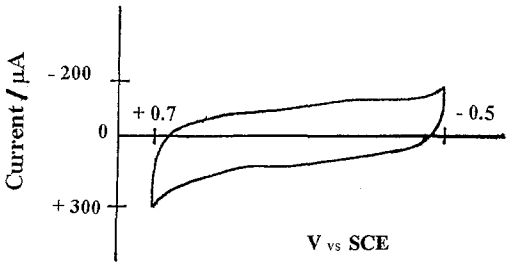

Fig. 2. Cyclic voltammogram of Mn(III)CyDTA on graphite, in 1 M KCl supporting electrolyte. Mn(III)CyDTA concentration of 0.092 mM, CyDTA/Mn molar ratio 2/1, pH 8.0, 25 °C. Scan rate $33\,mV\,s^{-1}$.

point of the complex, which is 1:1, causing the absence of the peak currents (Fig. 2).

However, an additional factor must be taken into account, which is the competition at pH > 7 between a water molecule and OH^- for the seventh coordination site of Mn(III). The following equilibrium reaction can be written:

$$[Mn(III)CyDTA(H_2O)]^- \xleftrightarrow{K_m} [Mn(III)CyDTA(OH^-)]^{2-} + H^+ \quad (1)$$

where the equilibrium constant K_m is equal to 7.76×10^{-9} mol dm^{-3} at 25 °C [14].

In alkaline media the equilibrium in Equation 1 is shifted toward the hydroxo species which is known to be inactive toward electron-transfer processes, due to the strong bonding by OH^- [29]. Thus, the absence of a cyclic voltammetry response in alkaline media can be partly attributed to the formation of the hydroxo species.

However, as shown in Fig. 3, when the supporting electrolyte contained 0.1 M $NaHCO_3$ in addition to 1 M KCl, the Mn(III)CyDTA revealed both anodic and cathodic peaks on the graphite electrode at pH 8.0. The HCO_3^- probably competes for the seventh coordination site of Mn(III) by forming the $[Mn(III)CyDTA(HCO_3^-)]^{2-}$ species. It is hypothesized that the presence of the bicarbonate ion in the coordination sphere of Mn(III) facilitates the electron-transfer process and brings about the cyclic voltammetry response.

Furthermore, increasing the scan rate above 67 mV s^{-1}, a second cathodic peak developed before the first, diffusion controlled peak (Fig. 3). This is called prepeak behaviour [30, 31] and is characteristic for the adsorption of the products of the reduction reaction, which are Mn(II) species (e.g. Mn(II)CyDTA, $Mn(OH)_2$).

Also, the cyclic voltammogram of Mn(III)CyDTA was recorded on both platinum and stainless steel electrodes at pH 10.0 in a 0.1 M $NaHCO_3$ + 1 M KCl supporting electrolyte (Fig. 4). Although, both electrodes showed prepeak behaviour, the separation of the adsorption controlled prepeak from the diffusion controlled peak was the most distinct on platinum. This qualitatively suggests a stronger adsorption on Pt than on stainless steel. The cathodic prepeak at −20 mV vs SCE belongs to the reduction of Mn(III)-CyDTA to adsorbed Mn(II) species, while on the reverse scan, the anodic prepeak at +180 mV vs SCE is due to the oxidation of the adsorption film (Fig. 4).

Other authors have also reported the adsorption of Mn(II) species during the electrolytic oxidation of Mn(II) under various conditions such as: pH 2 and 7

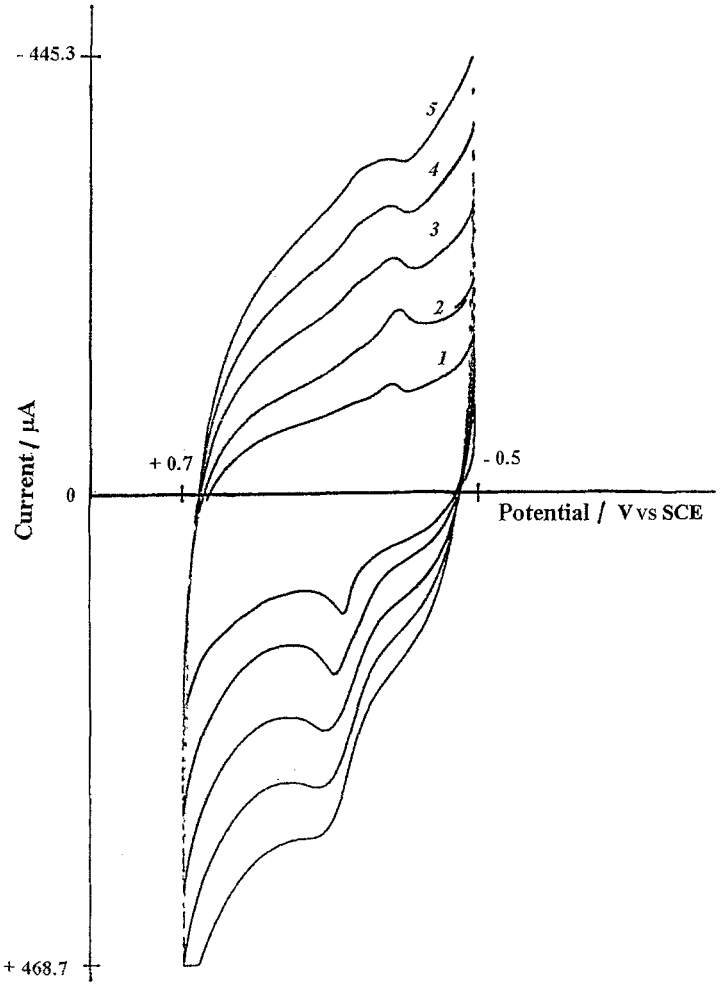

Fig. 3. Cyclic voltammogram of Mn(III)CyDTA on graphite, in a 1 M KCl + 0.1 M $NaHCO_3$ supporting electrolyte. Mn(III)CyDTA concentration of 0.092 mM, CyDTA/Mn molar ratio 2/1, pH 8.0, 25 °C. Key: scan rate (1) 33, (2) 67, (3) 100, (4) 133 and (5) 167 mV s^{-1}.

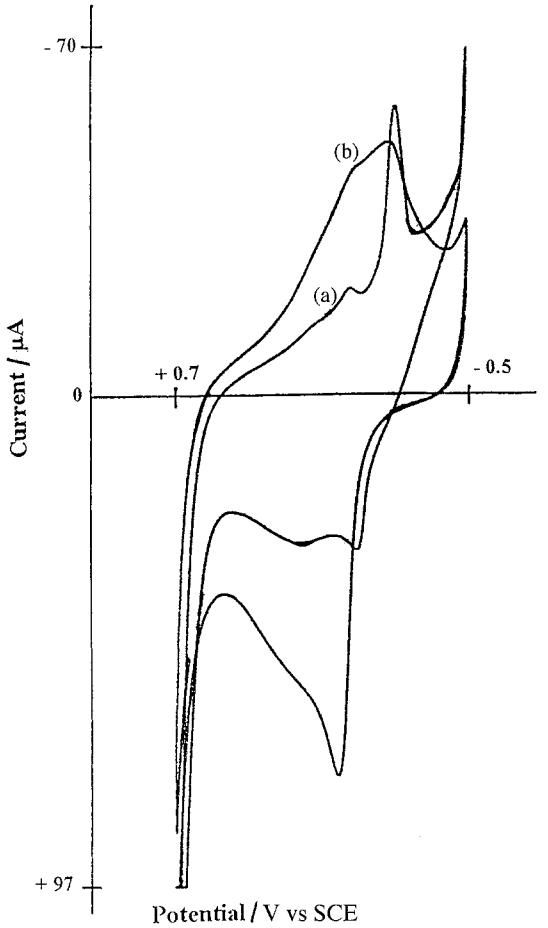

Fig. 4. Cyclic voltammogram of Mn(III)CyDTA on platinum and stainless steel. Supporting electrolyte: 1 M KCl + 0.1 M $NaHCO_3$, pH 10.0, 25 °C. Mn(III)CyDTA concentration of 0.092 mM, CyDTA/Mn molar ratio 2/1. Scan rate 33 mV s^{-1}. Key (a) Pt and (b) stainless steel.

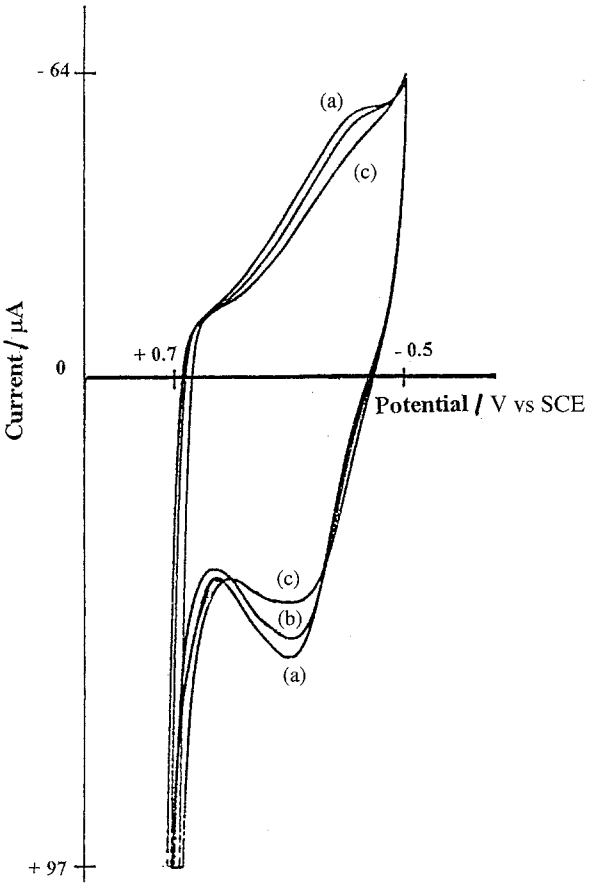

Fig. 5. Cyclic voltammogram of Mn(III)CyDTA on stainless steel as a function of pH. Supporting electrolyte 1 M KCl + 0.1 M $NaHCO_3$, 25 °C, Mn(III)CyDTA concentration of 0.092 mM, CyDTA/Mn molar ratio 2/1. Scan rate 67 mV s^{-1} Key: (a) pH 12.9, (b) pH 13.1 and (c) pH 13.4.

in both Na_2SO_4 and $Na_4P_2O_7$ medium on a platinum electrode [32–34], or in 6.15 M H_2SO_4 on a glassy carbon electrode [9].

The pH dependence of the Mn(III)CyDTA electrochemical behaviour was investigated in the pH range of 12.9 to 13.4 at 25 °C on the stainless steel electrode (Fig. 5). As can be seen from Fig. 5, increasing the pH generated a decrease in both the cathodic and anodic peak currents together with a shift of the cathodic peak potential toward more negative values, from −160 mV vs SCE at pH 10.0 (Fig. 4) to −244 mV vs SCE at pH 12.9 (Fig. 5). This is due to the parallel hydrolysis and disproportionation of Mn(III)CyDTA in strong alkaline media. At pH 13.4 the cathodic peak vanishes indicating a fast and complete decomposition of Mn(III)-CyDTA. The anodic peak is still present, but the oxidation of Mn(II)CyDTA became irreversible.

From the point of view of a further attempt to electrochemically generate Mn(III)CyDTA, the cyclic voltammetry experiments revealed a couple of important aspects. First of all the HCO_3^- had paramount importance in bringing about the cyclic voltammetry response of Mn(III)CyDTA. Furthermore, the adsorption of Mn(II) species can represent a problem during the electrosynthesis. Also, the pH of the electrolyte cannot exceed 11, in order to avoid the enhanced decomposition of the complex.

3.2. *Electrochemical generation of Mn(III)CyDTA in alkaline media*

For a proper interpretation of the results obtained during the electrolytic oxidation of Mn(II)CyDTA, it is important to know if or how much Mn(III)CyDTA is formed by a parallel, nonelectrochemical route. In alkaline solutions, in the presence of dissolved oxygen, the Mn(II)CyDTA might undergo spontaneous chemical oxidation to form Mn(III)CyDTA. Such reactions were described for Mn(II) complexes with sorbitol and gluconate [35, 36]. Thus, 'blank' synthesis runs (i.e., without current) were performed by mixing the anolyte under aerobic conditions for 1 h at pH 10.5, 25 °C, for two CyDTA/Mn molar ratio, 1/1 and 2/1, respectively. The results are presented in Fig. 6.

Figure 6 shows that for a 2/1 CyDTA/Mn molar ratio there was no measurable concentration of Mn(III)CyDTA formed by aerobic oxidation. However, for an equimolar CyDTA/Mn molar ratio, the concentration of aerobically produced Mn(III)CyDTA followed a parabolic shape as a function of Mn(II) concentration. It is thought that the increase, levelling and subsequent drop in the Mn(III)CyDTA concentration indicates a catalyst–inhibitor conversion of Mn(II)CyDTA in alkaline media, similar to the behaviour of the Mn(II) sorbitol

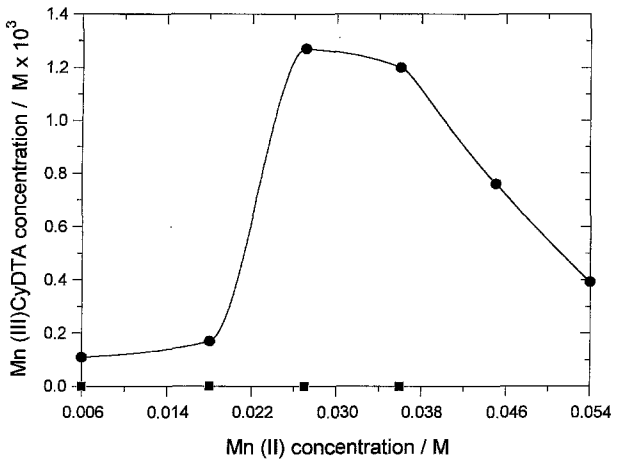

Fig. 6. Aerobic oxidation of Mn(II)CyDTA at pH 10.5, 25 °C. Reaction time 1 h. Key: CyDTA/Mn molar ratio (●) 1/1 and (■) 2/1.

complex at pH 12.1 [37]. The aerobic oxidation of Mn(II)CyDTA involves various oxygen containing free radical species. After exceeding an induction concentration of Mn(II), i.e. 18 mM (Fig. 6), the Mn(II) catalyses the oxygen reduction to form Mn(III) and hydrogen peroxide. However, at concentrations above 27 mM, both the Mn(II) and CyDTA act as sequestering agents, tying up and scavenging the free radicals (e.g., HO·, HOO·), thus the Mn(III) formation is inhibited and its concentration drops.

Consequently, in the case of the 1/1 CyDTA/Mn molar ratio, the Mn(III)CyDTA generated by aerobic oxidation has to be subtracted from the total Mn(III)CyDTA concentration in the anode chamber, to find the true current efficiency for electrochemical Mn(III) formation.

3.2.1. Stainless steel screen anode. The first anode investigated was the stainless steel screen. The total Mn(III)CyDTA concentration in the anode chamber and the current efficiency for Mn(III) after 1 h of electrosynthesis at a constant current density of 2.6 A m^{-2}, with an initial pH of 10.5 at 25 °C, is presented in Fig. 7.

As illustrated in Fig. 7 there are significant differences in the outcome of the electrosynthesis as a function of CyDTA/Mn molar ratio. To adequately discuss the mechanism of electrosynthesis based on Fig. 7, the role of the convective mass transfer due to both mechanical mixing and oxygen evolution at the anode has to be assessed. The limiting current density corresponding to the Mn(II)CyDTA oxidation in alkaline media was calculated according to the procedure described in the Appendix and it was compared with the measured current density for Mn(III) formation (Fig. 8).

Figure 8 shows that, over the entire range of explored Mn(II) concentration (6–54 mM), the limiting current density is about one and two order of magnitude higher than the actual current density for Mn(III), indicating that the electrosynthesis was not under convective mass transfer control. Thus, the results presented in Fig. 7, are determined by other

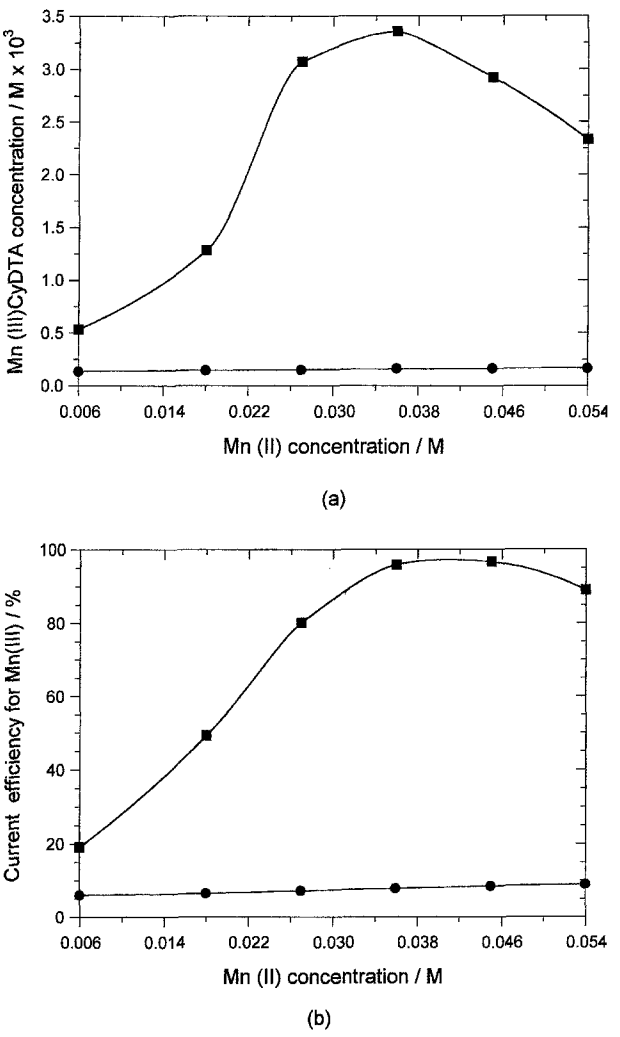

Fig. 7. Electrosynthesis of Mn(III)CyDTA on a stainless steel screen anode: the effect of Mn(II) concentration at a constant current density of 2.6 A m^{-2}. pH_{in} 10.5, 25 °C, 1 h. (a) Mn(III)CyDTA concentration, (b) current efficiency. Key: CyDTA/Mn molar ratio (■) 1/1 and (●) 2/1.

rate controlling steps (e.g., electrode kinetics, adsorption of Mn(II) species, mass transfer across the adsorbed layer).

Figure 7 indicates that, in the case of 1/1 CyDTA/Mn molar ratio, three different phases of the electrosynthesis exists. In the range of 6 to 36 mM Mn(II) concentration, the current efficiency for Mn(III) increases up to 96%. In the subsequent Mn(II) concentration range, from 36 to 45 mM, the current efficiency is levelled off at 96%, while at even higher reactant concentration the current efficiency for Mn(III) drops to 89%. This intricate behaviour is determined by the significant changes of the surface of the stainless steel screen anode.

Beginning with the 18 mM Mn(II) concentration, a visible, brownish deposit was formed on the anode. The anodic film modifies both the surface characteristics and the electrocatalytic properties of the stainless steel screen. At the end of the electrolysis the anolyte was acidified with glacial acetic acid as outlined in Section 2.3. Under mixing in acidic media, the anodic deposit was washed from the stainless steel screen surface, thus the analysed samples contained Mn(III)CyDTA from both the electrolyte and adsorbed layer.

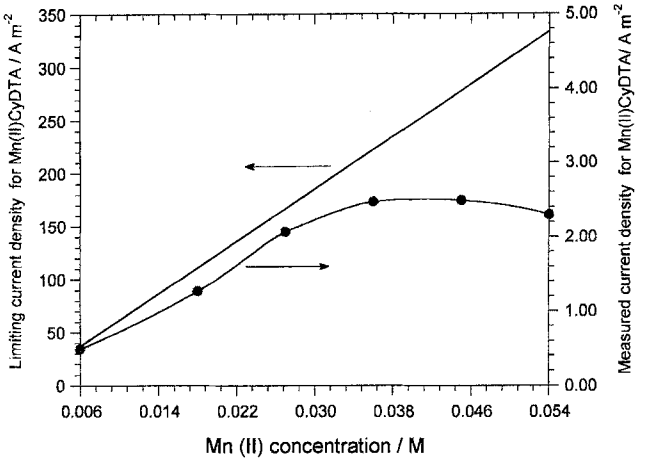

Fig. 8. Electrosynthesis of Mn(III)CyDTA on a stainless steel screen anode: the limiting and measured current densities for Mn(II) as a function of Mn(II) concentration for a constant total applied current density of 2.6 A m^{-2}. CyDTA/Mn molar ratio 1/1, pH_{in} 10.5, 25 °C. Key: (——) limiting current density, (●) measured current density.

In the range of 18 to 36 mM Mn(II) concentration the current efficiency for Mn(III) increases from 47% to 96% (Fig. 7), the electrosynthesis is kinetically controlled on a 'modified' stainless steel surface. For Mn(II) concentration above 36 mM, the anodic film is thick and the oxidation takes place almost entirely in the adsorbed layer through the interconversion of different adsorbed species which probably include Mn(II)CyDTA, $Mn(OH)_2$, MnOOH and MnO_2 [38].

Besides modifying the surface and electrochemical properties of the stainless steel, the thick anodic film hinders the transport of Mn(II) ions from the surface of the adsorbed layer to the electrode surface. This property of the anodic deposit can be observed in Fig. 7 for a 54 mM Mn(II) concentration, where the current efficiency for Mn(III) dropped from 96% to 89%. The electrosynthesis is controlled by the diffusion of Mn(II) through the thick anodic film.

When the CyDTA was in excess, 2/1 CyDTA/Mn molar ratio, the electrolytic oxidation of Mn(II)CyDTA behaved differently. There was no visible buildup of an anodic deposit at any of the explored concentrations; however, the current efficiency for Mn(III) was about 4 to 18 times lower than in the equimolar case (Fig. 7). Furthermore, the current efficiency for Mn(III) is virtually independent of the Mn(II) concentration, as long as the CyDTA/Mn molar ratio is 2/1 (i.e., apparent zero order kinetics). Consequently, a strong complexation of Mn(II) by an excess of CyDTA, does not favour the electrochemical generation of Mn(III)CyDTA. This leads to the conclusion that the actual reactant at the anode surface is rather the uncoordinated Mn(II) ion than the Mn(II)CyDTA itself. It is thought that in order to react, the Mn(II) must be free of the voluminous CyDTA ligand in the vicinity of the anode surface (i.e., inside the electric double layer).

In Fig. 9 the effect of current density on the current efficiency for Mn(III) formation is presented, for a constant Mn(II) concentration of 18 mM.

For an equimolar CyDTA/Mn ratio, an increase in current density from 2.6 to 5.8 A m^{-2}, brought about an increase of current efficiency for Mn(III) from 49% to 60%. However, increasing the current density above 5.8 A m^{-2} generated a dramatic drop of the current efficiency for Mn(III), from 60% to 3% at 15.5 A m^{-2} (Fig. 9). This is due also to the formation of a thick anodic film which blocks the transport of the Mn(II) to the anode surface. For an excess of CyDTA, again, there was no evidence of film formation at any of the explored current densities.

The data presented in Figs 7 and 9, show that the stainless steel screen can be employed as anode for Mn(III)CyDTA electrosynthesis at equimolar ligand to metal ratio only at low current density (<5.8 A m^{-2}) and low Mn(II) concentration (<18 mM), where the anodic deposition does not affect the process.

3.2.2. Comparison of various anode materials. To find a better anode for the electrolytic oxidation of Mn(II)CyDTA in alkaline media, which can function at higher current densities than 5.8 A m^{-2}, four additional materials were tested. These are: Pt/Ti, PbO_2/Pb, Ni and graphite plates. For comparison the results obtained on a stainless steel plate are

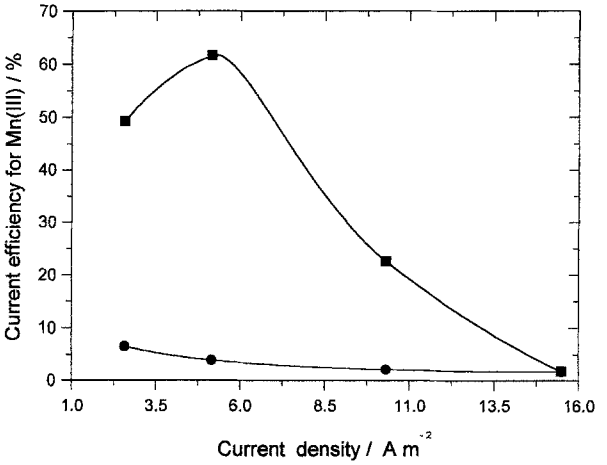

Fig. 9. Electrosynthesis of Mn(III)CyDTA on a stainless steel screen anode: the effect of current density on the current efficiency for Mn(III) at a constant Mn(II) concentration of 18 mM. pH_{in} 10.5, 25 °C, 1 h reaction time. Key: CyDTA/Mn molar ratio (■) 1/1 and (●) 2/1.

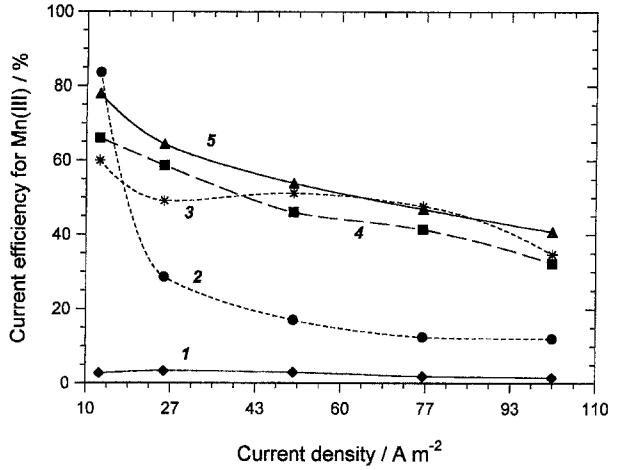

Fig. 10. Comparison among various anode plates: the effect of current density on the current efficiency for Mn(III) at a constant Mn(II) concentration of 18 mM. CyDTA/Mn molar ratio 1/1, pH_{in} 10.5, 25 °C, 1 h. Key: anode (◆) stainless steel, (●) Ni, (*) PbO_2/Pb, (■) Pt/Ti and (▲) graphite.

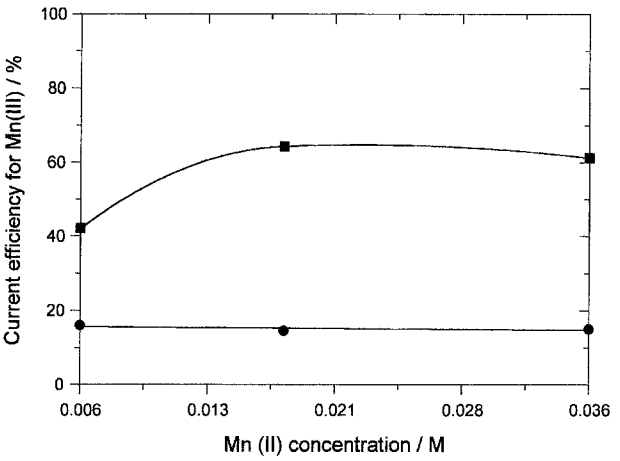

Fig. 11. Electrosynthesis of Mn(III)CyDTA on a graphite plate anode: the effect of Mn(II) concentration on the current efficiency at a constant current density of 25 A m^{-2}. pH_{in} 10.5, 25 °C, 1 h. Key: CyDTA/Mn molar ratio (■) 1/1 and (●) 2/1.

presented as well. In all runs equimolar concentration of 18 mM Mn(II) and CyDTA were employed. The initial pH was 10.5 and the temperature 25 °C. The cumulative current efficiency for Mn(III) as a function of current density over 1 h reaction time is presented in Fig. 10.

As can be seen from Fig. 10, among the five anodes, graphite gave the highest current efficiency for Mn(III), between 65% and 41% for current densities from 25 to 102 A m^{-2}. Interestingly, there was no indication of anodic deposit formation on graphite.

The nickel anode had a peculiar behaviour. At the lowest explored current density (i.e., 13 A m^{-2}) it gave the highest current efficiency for Mn(III), i.e. 84% (Fig. 10). Although, there was no brownish deposit formation on nickel as well, at current densities above 13 A m^{-2}, the current efficiency for Mn(III) dropped below 30% and the initially silvery nickel anode turned rapidly dark grey due to the formation of nickel hydroxides and oxides on its surface. This had an important effect on the kinetics of the electrosynthesis, causing the marked drop of current efficiency for Mn(III) formation.

The Pt/Ti plate gave current efficiencies for Mn(III) between 32% and 66%, without an anodic film formation.

The PbO_2/Pb anode, recommended for the anodic oxidation of Mn(II) in strong acidic media [4], was found to be less useful for the present system. Over the entire range of current densities an anodic layer was formed on its surface, which was washed off with great difficulty in acidic media.

Based on the results presented in Fig. 10, the graphite was subjected to further investigations.

3.2.3. Graphite plate anode. Although there was no anodic film formation on graphite for an 18 mM Mn(II) concentration (Fig. 10), it was suspected that at higher Mn(II) concentration adsorption on the porous structure of the graphite might occur, deteriorating its performance as an anode in the present system.

Indeed, Fig. 11 clearly shows that for Mn(II) concentration above 18 mM, the current efficiency for Mn(III) slightly drops, from 65% at 18 mM to 60% at 36 mM, as a result of deposit formation.

Again, in the case of an excess CyDTA, there was no sign of deposit formation, the current efficiency levelled off at 15%.

By increasing the current density, at a Mn(II) concentration of 6 mM, the Mn(III)CyDTA concentration increases for both CyDTA/Mn molar ratios (Fig. 12). After 1 h reaction time at 102 A m^{-2} anode current density, for a 1/1 CyDTA/Mn molar ratio, the yield of Mn(III) was 63% with an 18% current efficiency (Fig. 12).

3.2.4. The influence of pH and the importance of pH control during Mn(III)CyDTA electrosynthesis in alkaline media. The idea that the actual reactant at the anode surface is rather the uncoordinated Mn(II) (Section 3.2.1), is further supported by the effect of pH on the electrosynthesis of Mn(III)CyDTA (Fig. 13). The complexation by CyDTA is stronger at pH 9.0 than at pH 10.5, making more difficult the dissociation of the complex to form the uncoordinated Mn(II) in the vicinity of the anode surface. Consequently, the electrochemical oxidation of Mn(II)CyDTA is less efficient at pH 9.0 than at pH 10.5, which is illustrated by about three times lower Mn(III)CyDTA concentration at pH 9.0 vs pH 10.5 (Fig. 13).

The upper limit of the operational pH is determined by the stability of the complex and cannot exceed a value of 11 at 25 °C [17, 21].

Due to the parallel oxygen evolution on the anode, the pH of the anolyte decreases during the electrosynthesis of Mn(III)CyDTA, from 10.5 initially, to about 8.8 if the electrosynthesis is prolonged to 3 h (Fig. 14).

Figure 15 shows that the uncontrolled decrease of pH has a negative effect on the electrosynthesis on a graphite anode, especially over a 3 h reaction period. Considering that the measured Mn(III)CyDTA

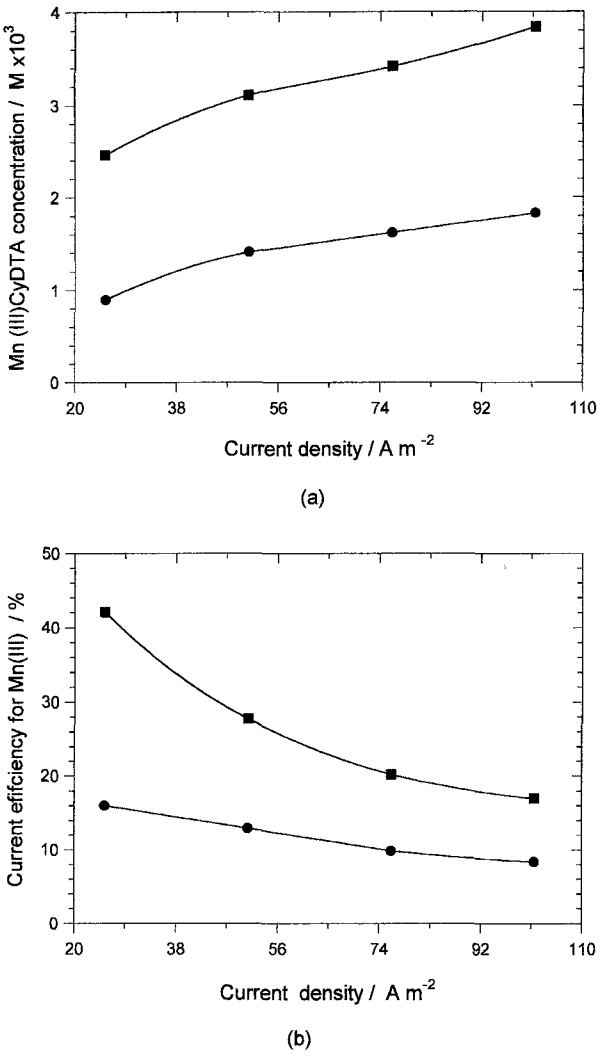

Fig. 12. Electrosynthesis of Mn(III)CyDTA on a graphite plate anode: the effect of current density at a constant Mn(II) concentration of 6 mM. pH_{in} 10.5, 25 °C, 1 h. (a) Mn(III)CyDTA concentration, (b) current efficiency. Key: CyDTA/Mn molar ratio (■) 1/1 and (●) 2/1.

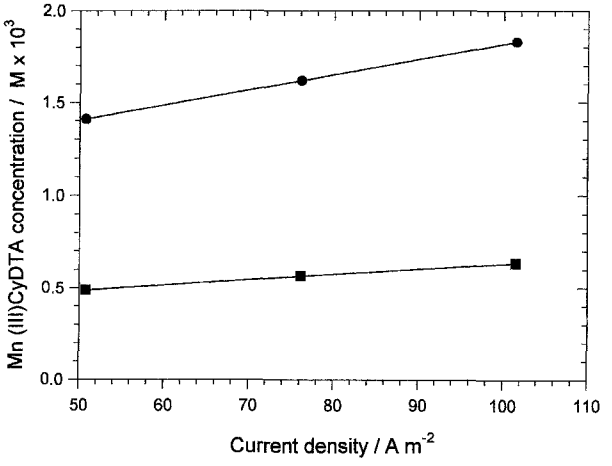

Fig. 13. The effect of pH on the electrosynthesis of Mn(III)CyDTA: the Mn(III)CyDTA concentration as a function of current density at a constant Mn(II) concentration of 6 mM. Graphite plate anode, CyDTA/Mn molar ratio 2/1, 25 °C, 1 h. Key: (●) pH 10.5 and (■) pH 9.0.

concentration is the net, accumulated Mn(III)CyDTA (i.e., electrochemically produced minus decomposed), in the absence of pH control, beyond 1 h, the

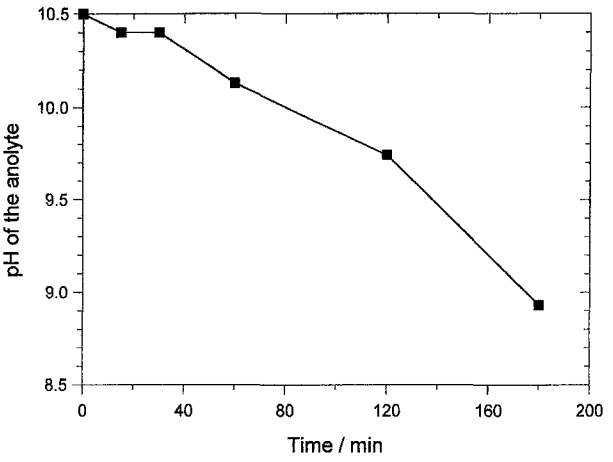

Fig. 14. The pH profile of the anolyte during Mn(III)CyDTA electrosynthesis on a graphite plate anode at a constant current density of 51 A m^{-2} and at a constant Mn(II) concentration of 6 mM. CyDTA/Mn molar ratio 2/1, 25 °C.

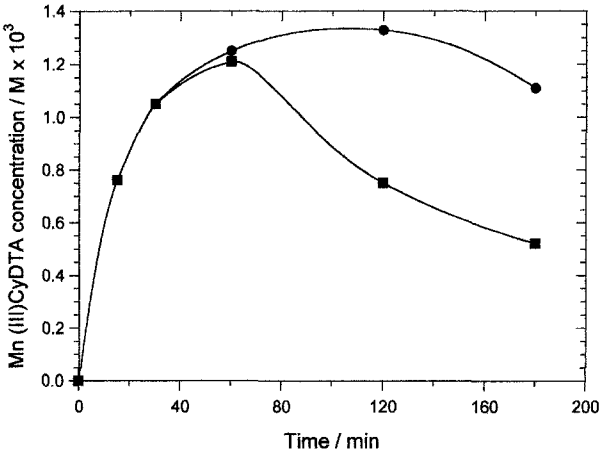

Fig. 15. The effect of pH control at 10.5 on the electrosynthesis of Mn(III)CyDTA on a graphite plate anode at a constant current density of 51 A m^{-2} and at a Mn(II) concentration of 6 mM, CyDTA/Mn molar ratio 2/1, 25 °C. Key: (●) with pH control at 10.5 and (■) without pH control.

decomposition exceeds the electrochemical generation, due to a slower electrolytic oxidation of Mn(II)-CyDTA at pH below 10.0. To maintain a high, 1.35 mM Mn(II)CyDTA concentration, over a 2 h reaction time, the pH of the anolyte was kept constant at 10.5, according to the procedure described in Section 2.2. Even with pH control at 10.5, after 3 h, the Mn(III)-CyDTA concentration diminished, due to the clogging of the porous graphite structure by the anodic deposit, causing a deterioration of the electrochemical performance.

4. Conclusions

A manganese aminopolycarboxylate complex (i.e., Mn(III)CyDTA) was electrochemically generated in alkaline media, at pH 9.0 and 10.5, respectively, from Mn(II)CyDTA (6–54 mM) for two CyDTA/Mn molar ratios, 1/1 and 2/1. A divided batch electrochemical reactor was employed with current densities from 2.6 to 102 A m^{-2}.

The cyclic voltammetry experiments showed the importance of the HCO_3^- ion (0.1 M) in bringing about

the peak responses of Mn(III)CyDTA in alkaline media, at a 2/1 CyDTA/Mn molar ratio. It is thought that the HCO_3^- ion competes with the HO^- ion for the seventh coordination site of Mn(III), by forming the $[Mn(III)CyDTA(HCO_3)]^{2-}$ species, which is more active in electron-transfer processes than the hydroxo form (i.e., $[Mn(III)CyDTA(HO)]^{2-}$). However, more studies are required to clearly establish the role of the HCO_3^- ion or to search for other anions with similar effect.

The cyclic voltammograms on graphite, platinum and stainless steel, were consistent with a prepeak behaviour, due to the adsorption of the Mn(II) species.

During the electrolytic oxidation of Mn(II)CyDTA, for an equimolar ligand to metal ratio, depending on the anode material, Mn(II) concentration and current density, a brownish deposition occurred on the anode surface. The anodic layer modified both the electrochemical properties of the electrode and hindered the transport of Mn(II) ions to the anode surface. Due to this dual behaviour, the anodic deposit is sometimes called a 'bifunctional electrochemical system' [39].

When the CyDTA was in excess (i.e., CyDTA/Mn 2/1 molar ratio), there was no brownish deposit formation on any of the anodes, indicating that strong complexation of Mn(II) prevented the build up of manganese hydroxides and oxides on the anode surface. However, for a 2/1 CyDTA/Mn molar ratio, the current efficiency for Mn(III) is considerably lower than in the equimolar situation. This observation together with the fact that the electrosynthesis is favoured by pH 10.5 vs pH 9.0, indicates that under conditions which destabilize the Mn(II)CyDTA, the electrolytic oxidation of the complex occurs more readily. This leads to the conclusion that in the vicinity of the anode, inside the electric double layer, the Mn(II) ion must be free of the voluminous CyDTA ligand (resemblance with the inner-sphere mechanism for homogeneous electron-transfer reactions [1]).

An additional aspect which should be taken into account in interpreting the results, is the possibility of CyDTA oxidation at the anode, with the formation of an adsorbed organic film. The organic anodic film can contribute also to the loss of current efficiency for Mn(III). Such phenomena were described for the oxidation of Mn(II) in 88% H_2SO_4 on a platinum anode in the presence of organic acids such as benzoic acid and aliphatic diacids [2]. More investigations are needed to clarify this aspect as well.

Regarding the employed anodes, graphite gave the highest current efficiency for Mn(III) without visible evidence of anodic deposition, 78% at $13\,A\,m^{-2}$. However, over extended reaction times, beyond 2 h, deposition of a brownish layer occurred, causing a less efficient electrochemical synthesis of Mn(III)CyDTA. Platinized titanium was free also of an anodic adsorption layer after a 1 h reaction time, but the current efficiency for Mn(III) was lower than on graphite (i.e., 66% at $13\,A\,m^{-2}$). The stainless steel screen can be employed without anodic film formation only at low current density ($<5.8\,A\,m^{-2}$) and low Mn(II) concentration (<18 mM). Both PbO_2/Pb and nickel anodes were found unsuitable for the electrolytic oxidation of Mn(II)CyDTA in alkaline media. On PbO_2/Pb, a thick anodic deposit was formed, being very difficult to remove from the electrode surface.

The electrochemically generated Mn(III)CyDTA can be easily recovered from alkaline media by acidification. From the acidic solution, the solid Mn(III)CyDTA can be separated by crystallization [17]. Furthermore, the electrochemical method is convenient for subsequent electrochemically mediated oxidations in alkaline media. Recently, a procedure for *in situ* electrochemically mediated oxygen delignification of wood pulp was developed, based on the electrosynthesis of Mn(III)CyDTA in alkaline media [21, 40].

Acknowledgement

The authors would like to thank the Pulp and Paper Research Institute of Canada (Paprican) for the generous financial support.

References

[1] F. A. Cotton and G. Wilkinson, 'Advanced Inorganic Chemistry', 5th edn., J. Wiley & Sons, New York (1988).
[2] Ch. Comninellis, Ch. Griessen and E. Plattner, *J. Electrochem. Soc.* **132** (1985) 72.
[3] R. Ramaswamy, M. S. Venkatachalapathy and H. V. K. Udupa, *ibid.* **110** (1963) 202.
[4] J. Y. Welsh, *Electrochem. Technol.* **5**(11, 12) (1967) 504.
[5] Ch. Comninellis and E. Plattner, *J. Electrochem. Soc.* **129** (1982) 749.
[6] *Idem, J. Appl. Electrochem.* **14** (1984) 533.
[7] M. S. Venkatachalapathy, R. Ramaswamy and H. V. K. Udupa, *Bull. Acad. Polon. Sci.* **6** (1958) 487.
[8] G. A. Kokarev, M. Ya. Fioshin, E. V. Gromova and A. T. Sorokovykh, *Soviet Electrochem.* **17** (1981) 1140.
[9] A. T. Kuhn and T. H. Randle, *J. Chem. Soc. Faraday Trans.* **79** (1983) 417.
[10] J. C. Hunter and A. Koziawa, 'Manganese Technetium, and Ruthenium', in 'Standard Potentials in Aqueous Solution' (edited by A. J. Bard, R. Parsons and J. Jordan), Marcel Dekker, New York (1985).
[11] Y. S. Perng, PhD. thesis, Department of Chemical Engineering, University of British Columbia, Vancouver (1993).
[12] Y. S. Perng, C. W. Oloman and B. R. James, *Tappi J.* **76**(10) (1993) 139.
[13] Y. S. Perng and C. W. Oloman, *ibid.* **77**(7) (1994) 119.
[14] S. Gangopadhyay, M. Ali, A. Dutta and P. Banerjee, *J. Chem. Soc. Dalton Trans.* (1994) 841.
[15] J. Peinado, F. Toribio and D. Perez-Bendito, *Analyst* **112** (1987) 771.
[16] Y. S. Perng, C. W. Oloman, P. A. Watson and B. R. James, *Tappi J.* **77**(11) (1994) 119.
[17] R. E. Hamm and M. A. Suwyn, *Inorg. Chem.* **6** (1967) 139.
[18] R. J. Day and C. N. Reilley, *Anal. Chem.* **37** (1965) 1326.
[19] H. Gampp, *ibid.* **59** (1987) 2456.
[20] M. A. Suwyn and R. E. Hamm, *Inorg. Chem.* **6** (1967) 142.
[21] E. L. Gyenge, MASc. thesis, Department of Chemical Engineering, University of British Columbia, Vancouver (1995).
[22] F. Cui and D. Dolphin, *Holzforschung* **44** (1990) 279.
[23] I. K. Bhat and B. S. Sherigara, *Trans. Metal Chem.* **19** (1994) 178.
[24] E. Gileadi, E. Kirowa-Eisner and J. Penciner, 'Interfacial Electrochemistry. An Experimental Approach', Addison-Wesley, Reading, MA (1975).
[25] R. Pribl and J. Horacek, *Collect. Czech. Chem. Comm.* **14** (1949) 626.

[26] A. I. Vogel, 'Textbook of Quantitative Inorganic Analysis', Longman, New York (1978).
[27] L. L. Landucci, *Tappi J.* **62**(4) (1979) 71.
[28] L. Piszczek, A. Ignatowicz and J. Kielbasa, *J. Chem. Ed.* **65** (1988) 171.
[29] S. Gangopadhyay, M. Ali and P. Banerjee, *Bull. Chem. Soc. Jpn.* **65** (1992) 517.
[30] A. J. Bard and L. R. Faulkner, 'Electrochemical Methods. Fundamentals and Applications', J. Wiley & Sons, New York (1980).
[31] E. R. Brown and J. R. Sandifer, 'Cyclic Voltammetry, AC Polarography and Related Techniques', *in* 'Physical Methods of Chemistry', 2nd edn, vol. II, 'Electrochemical Methods' (ed. by B. W. Rossiter and J. E. Hamilton), J. Wiley & Sons, New York (1986).
[32] J. E. Harrar and L. P. Rigdon, *Anal. Chem.* **41** (1969) 763.
[33] S. V. Gorbachev and V. A. Belyaeva, *Russ. J. Phys. Chem.* **36** (1962) 114.
[34] *Idem, ibid.* **37** (1963) 97.
[35] M. E. Bodini and D. T. Sawyer, *J. Am. Chem. Soc.* **98**(26) (1976) 8366.
[36] D. T. Richens, C. G. Smith and D. T. Sawyer, *Inorg. Chem.* **18** (1979) 706.
[37] Ph. K. Lim, J. A. Cha and B. S. Fagg, *Ind. Eng. Chem. Fundam.* **23** (1984) 29.
[38] A. M. Sukhotin and I. G. Osipenkova, *J. Gen. Chem. of USSR* **51** (1978) 805.
[39] N. D. Ivanova and S. V. Ivanov, *Russ. Chem. Rev.* **62** (1993) 907.
[40] E. L. Gyenge and C. W. Oloman, accepted for publication in *Tappi J.*, November 1995.
[41] J. A. Dean, 'Lange's Handbook of Chemistry', 14th edn, McGraw-Hill, New York (1992).
[42] 'Perry's Chemical Engineers Handbook' (edited by R. H. Perry, D. W. Green and J. O. Maloney) 6th edn, McGraw-Hill, New York (1984).
[43] G. Prentice, 'Electrochemical Engineering Principles', Prentice Hall, Englewood Cliffs, NJ (1991).
[44] K. Stephan and H. Vogt, *Electrochim. Acta* **24** (1979) 11.
[45] T. Mizushina, R. Ito, S. Hiraoka, A. Ibususki and I. Sakaguchi, *J. Chem. Eng. Jpn.* **2** (1969) 89.
[46] J. R. Selman and Ch. W. Tobias, 'Mass-Transfer Measurements by the Limiting-Current Technique', *in* 'Advances in Chemical Engineering', vol. 10 (edited by Th. B. Drew), Academic Press, New York (1978).
[47] G. H. Sedahmed and L. W. Shemilt, *J. Appl. Electrochem.* **14** (1984) 123.

Appendix: Calculation of the limiting current density for Mn(II)CyDTA oxidation on a stainless steel screen anode

Physico-chemical data:

Limiting equivalent conductance of Mn(II) in aqueous solution at 25 °C: $\lambda^{\circ}_{Mn(II)} = 53.5 \times 10^{-4}\ S\,m^2\,equiv^{-1}$ [41].

Limiting equivalent conductance of CyDTA in aqueous solution at 25 °C: (approximated with the value for the cyclohexane carboxylate anion) $\lambda^{\circ}_{CyDTA} = 28.7 \times 10^{-4}\ S\,m^2\,equiv^{-1}$ [41].

Electrolyte dynamic viscosity at 25 °C: $\mu = 9.5 \times 10^{-4}$ Pa s [42].

Electrolyte density at 25 °C: $\rho = 10^3\ kg\,m^{-3}$ [42].

Stainless steel screen anode area: $A = 232 \times 10^{-4}\ m^2$.

Impeller diameter: $d = 4.4 \times 10^{-2}$ m.

Mixer rotation rate: $\omega = 47$ rps.

(a) *Estimation of the Mn(II)CyDTA diffusion coefficient at 25 °C*

According to the equation for the diffusion coefficient of a binary electrolyte in dilute aqueous solution [43], the diffusion coefficient of Mn(II)CyDTA at infinite dilution is given by

$$D^{\circ}_{Mn(II)CyDTA} = \frac{z_{Mn(II)}\lambda^{\circ}_{Mn(II)}D^{\circ}_{CyDTA} + |z_{CyDTA}|\lambda^{\circ}_{CyDTA}D^{\circ}_{Mn(II)}}{z_{Mn(II)}\lambda^{\circ}_{Mn(II)} + |z_{CyDTA}|\lambda^{\circ}_{CyDTA}} \quad (A1)$$

The diffusion coefficients at infinite dilution for both Mn(II) and CyDTA can be calculated from the Nernst–Einstein equation:

$$D^{\circ}_i = \lambda^{\circ}_i \frac{RT}{|z_i|F^2} \quad (A2)$$

where i is Mn(II) or CyDTA.

Substituting the numerical values in Equations A2 and A1 we have $D^{\circ}_{Mn(II)} = 7.1 \times 10^{-10}\ m^2\,s^{-1}$, $D^{\circ}_{CyDTA} = 1.9 \times 10^{-10}\ m^2\,s^{-1}$ and $D^{\circ}_{Mn(II)CyDTA} = 4.6 \times 10^{-10}\ m^2\,s^{-1}$.

In the present work the employed Mn(II)CyDTA concentration is between 6 and 54 mM. In the absence of a better approximation than the 'infinite dilution' one, it is assumed that the value for the diffusion coefficient of Mn(II)CyDTA calculated above, is still valid in the range of employed concentrations.

Thus, $D_{Mn(II)CyDTA} \sim D^{\circ}_{Mn(II)CyDTA}$.

(b) *Calculation of the total mass transfer coefficient*

The total mass transfer coefficient K_m due to both forced convection $K_{m,f}$ and electrolytic gas evolution $K_{m,g}$, is given by [44]

$$K_m = K_{m,f}\left[1 + \left(\frac{K_{m,g}}{K_{m,f}}\right)^2\right]^{1/2} \quad (A3)$$

The convective mass transfer coefficient $K_{m,f}$, for flow to the vertical screen anode in a cylindrical cell with an axial flow impeller (Section 2.2) is estimated by [45, 46]:

$$Sh = 0.228\,Re^{2/3}Sc^{1/3} \quad (A4)$$

where $Re = \omega d^2\rho/\mu$, $Sc = \mu/\rho D_{Mn(II)CyDTA}$ and $Sh = K_{m,f}d/D_{Mn(II)CyDTA}$.

By substituting the numerical values in Equation A4, we have $K_{m,f} = 6.4 \times 10^{-5}\ m\,s^{-1}$.

The mass transfer coefficient due to the anodic oxygen evolution on a stainless steel screen $K_{m,g}$, is given by [47]

$$K_{m,g} = 3.228 \times 10^{-5} \times (\dot{V}_g)^{0.469} \quad (A5)$$

In Equation A5 $\dot{V}_g$ is the volumetric oxygen discharge rate per unit electrode area ($cm^3\,cm^{-2}\,min^{-1}$) and $K_{m,g}$ is expressed in $m\,s^{-1}$. The volumetric oxygen discharge rate per unit electrode area can be calculated by combining Faraday's law with the gas law and the following expression results [21]:

$$\dot{V}_g = \frac{3.802 \times (1 - CE) \times I}{A} \quad (A6)$$

where CE is the current efficiency for Mn(III) formation, I the total applied current and A the stainless steel screen area.

Under the employed conditions, for CE from 19 to 96%, $K_{m_i g}$ is between $1.1 \times 10^{-6}\,m\,s^{-1}$ and $2.8 \times 10^{-7}\,m\,s^{-1}$. Thus, from Equation A3 the total mass transfer coefficient K_m is equal to $6.4 \times 10^{-5}\,m\,s^{-1}$, consequently, the mass transfer enhancement due to the anodic oxygen evolution had an insignificant effect on the overall mass transfer coefficient.

(c) *Calculation of the limiting current density*

The limiting current density for the Mn(II)CyDTA electrolytic oxidation is

$$i_L = zFK_m c_{Mn(II)CyDTA} \qquad (A7)$$

Substituting the numerical values in Equation A7, the limiting current density for the Mn(II)CyDTA oxidation is between $37\,A\,m^{-2}$ at 6 mM Mn(II)CyDTA and $333.5\,A\,m^{-2}$ at 54 mM Mn(II)CyDTA. These values were plotted in Fig. 8.